

Organometallic synthesis and characterization of CdSe quantum dots

KIRSTEN ENTZ

Department of Chemistry and Chemical Biology, McMaster University, Hamilton, ON, Canada; entzk@mcmaster.ca*

ABSTRACT: In this experiment, CdSe QDs were synthesized using a kinetic growth colloidal method in which selenide trioctylphosphine was injected into a precursor solution of CdO and surfactants at 250 °C. Nine fractions of the QDs were withdrawn from 5-180 seconds, resulting in a gradient of colloids from yellow to dark orange that ranged in average radius from 2.20 to 3.77 nm with a wide size distribution, as measured from transmission electron microscopy (TEM) images. Absorbance and emission spectra of these samples revealed that peak maxima positions increase with increasing QD sizes, and Stokes shifts ranged from 16-40 nm, decreasing over time. Spectral observations were rationalized using the particle-in-a-box theory, which suggests that narrower boxes have higher energy gaps between ground and excited states, thus higher energy light is absorbed/emitted by the smaller CdSe particles. The *d*-spacing of three CdSe colloids was 1.6, 1.6, and 1.8 Å as determined by the fast Fourier transform of the high-resolution TEM image.

INTRODUCTION

Semiconducting nanocrystals that exhibit quantum size effects in their optical and electronic properties are known as quantum dots (QDs), and their wide range of applications make them very important nanoscale materials. Some applications include light-emitting diodes in displays, photoconductors, and biosensors.¹ In particular, cadmium chalcogenides, including CdS, CdSe, and CdTe, have become widely investigated for their potential applications as biological fluorescent labels due to their size-tunable optical properties.² Properties of these QDs include bright luminescence, narrow emission peaks, and high photostability.³ Control of QD size and shape is important for QD applications, thus efforts have been made to produce CdSe QDs with narrow size distributions.¹

In QDs, an electron-hole pair (exciton), generated by excitation, is confined within its volume. This is known as quantum confinement in three dimensions. The size of the semiconductor particle must be less than double the Bohr radius of the excitons to experience quantum confinement. CdSe has a relatively large Bohr radius of 5.6 nm, which allows for a broad range of QD sizes to be observed.³ The size of CdSe quantum dots can be investigated using transmission electron microscopy (TEM). In this technique, a beam of electrons is passed through a sample, and an image is formed through this electron-sample interaction. TEM can also be used to understand the crystal structure of QDs, such as spacing between planes of atoms. CdSe quantum dots typically exist with the wurtzite or zincblende crystal structures. These crystal structures are very similar, however, zincblende lacks the inversion symmetry that the wurtzite structure has, thus resulting in different optical properties.⁴

Herein the synthesis of CdSe colloidal quantum dots and their spectrophotometric and microscopic characterization of CdSe colloidal quantum dots is reported and analyzed.

RESULTS AND DISCUSSION

Preparation of CdSe QDs

CdSe QDs were synthesized from CdO and elemental Se using a kinetic growth method wherein particle size depends on reaction time. The Cd precursor was prepared by dissolving CdO in a high-boiling point non-coordinating solvent, octadecene, with surfactants oleic acid and trioctylphosphine (TOP). Oleic acid is the surface-binding ligand to stabilize the nanocrystals and the cationic precursor. CdO formed a cadmium oleate complex once dissolved

in oleic acid, and the red/brown solution was heated to 250 °C. The Cd²⁺ ions are isolated in this solution. Metallic selenium powder was dissolved in octadecene with TOP, which coordinates to Se. TOP helps the Se dissolve and coats the QDs when they are made. The Se-TOP solution was injected into the cadmium precursor, inducing nucleation and growth of the nanoparticles. Se-TOP bonds break to release Se²⁻ ions which begin to react with Cd²⁺, and CdSe dots form and grow over time with a ligand shell around them. Nine fractions of the CdSe colloids were withdrawn from 5-180 seconds, as timed from the instant the selenium was added to the cadmium precursor. The aliquots from 5-30 seconds were removed from the reaction flask every 5 seconds, and the final 3 aliquots were removed at 60, 120, and 180 seconds. The fractions displayed a gradient of yellow to dark orange, with lighter colours observed in fractions collected at earlier reaction times (Figure 1). Blue luminescence of the first sample was observed under short-wave ultraviolet radiation.

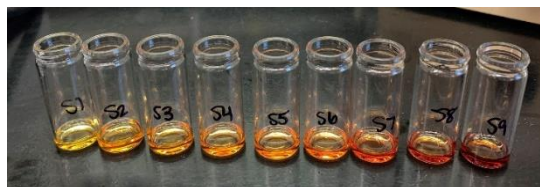


Figure 1. Photograph of nine fractions of colloidal suspensions of CdSe QDs. S1-9 were collected from 5-180 seconds.

In this reaction, CdSe is produced in the form of nanocrystals through a colloidal method, which can produce large quantities of nanocrystals with control of size and shape.⁵ A key difference between synthesizing a bulk crystal and a nanocrystal pertains to surface coordination due to the high surface-to-volume ratio of nanoparticles.^{4,6} The surface atoms of the CdSe nanoparticles are the dominant contribution to the physical and chemical properties of the semiconductors.⁷ Control of the size of the CdSe crystal is dominated by the ligand bonds with the surface ions of the nanocrystals. In order to create nanocrystals with a narrow size distribution, the nucleation step must be separated from the growth of the nanocrystal, which is achieved by injecting room temperature organometallic precursor TOP-Se into the hot surfactant solution.⁵ Previous methods to form CdSe used starting materials dimethylcadmium and bis(trimethylsilyl)selenium, which are very toxic and air-sensitive.⁸ Using CdCl₂ as a cadmium precursor instead of CdO in

dichloroethane results in the bulk precipitation of CdSe rather than a colloidal dispersion.⁹ Bulk crystalline CdSe can be prepared by the reaction between a metal salt and sodium or hydrogen selenide, or the reaction between Cd metal powder and elemental Se in an autoclave.¹⁰

Spectrophotometric Characterization of CdSe Colloids

CdSe QDs exemplify quantum confinement due to their restricted sizes, thus energy levels become discrete and only specific quantities of energy are absorbed. The spectrophotometric characterization of CdSe QDs can be described using the particle-in-a-box model, in which the QD is the box and the delocalized electrons and holes from the semiconductor are the particles. When the size of the QDs is smaller, the spacing between discrete energy levels is larger, thus smaller CdSe QDs absorb and emit light at shorter wavelengths (higher energy). As the dots increase in size, the spacing between energy levels decreases and lower energy light (longer wavelengths) is absorbed/emitted. Thus, there is a red shift as the CdSe QDs increase in size as the reaction time progresses. The particle-in-a-box model works well for understanding the size-dependent properties and spectrophotometric observations because the electrons cannot leave the semiconductor, however, it is a one-dimensional problem, so the particle-in-a-sphere more accurately applies to QDs. The equation relating energy gap and QD radius (Brus equation) is based on the particle-in-a-sphere model, but it only works well for larger QDs because it uses the individual effective mass of an electron and the hole as an approximation, thus overestimating the size of smaller QDs.³

Each of the nine CdSe colloid fractions were characterized by absorbance and emission spectrophotometry, and the results are summarized in Table 1.

Table 1. Absorbance and Emission Peak Positions and Stokes Shifts for CdSe QD Samples.

Sample	Withdraw Time (s)	Emission	Absorbance	Stokes Shift (nm)
		λ max (nm)	λ max (nm)	
1	5	546.02	506.00	40.02
2	10	558.05	530.00	28.05
3	15	567.94	538.00	29.94
4	20	572.05	548.00	24.05
5	25	580.00	554.00	26.00
6	30	582.05	560.00	22.05
7	60	592.05	570.00	22.05
8	120	596.02	580.00	16.02
9	180	604.05	586.00	18.05

For the absorbance spectra (Figure S1), the local maximum absorbance shifts from 506 nm in Sample 1 to 586 nm in Sample 9. This shift to longer wavelengths can be explained by the larger gap between energy levels when the QDs are smaller. Higher energy (shorter wavelength) light is absorbed by the QDs with larger energy gaps between their valence and conduction bands. Since this gap decreases as the QDs increase in size throughout the reaction, the wavelength of light absorbed increases. There is a large shift in λ_{max} for the first two samples because the size of the QDs increases logarithmically over time, thus the size is increasing more rapidly in samples withdrawn at earlier reaction times. This is also why the first five samples were withdrawn with five seconds in between. Additionally, the peaks are not well-defined for early samples because these colloids consist of very small nanocrystals. A similar trend was

observed for the emission spectra of the colloid samples (Figure S2). The local maximum emission wavelength was at 546.02 nm for Sample 1, and this maximum wavelength increased for the remaining samples up to 604.05 nm for Sample 9.

The Stokes shift is the difference between the wavelength of light absorbed and emitted for an excitation/relaxation electronic transition. It originates from George Gabirel Stokes, who studied fluorescence and found that the fluorescence emission occurs at a longer wavelength than the incident light. Absorbance and emission peak positions increase for larger CdSe colloids. Since the energy gap decreases between excited and ground states decreases with larger QD size, the absorbance and emission light energies also decrease. Upon radiation, electrons absorb light and move to an excited state of higher energy. When electrons relax, some energy is released non-radiatively, and then photons are emitted as the electrons relax back to the ground state. The QDs absorb more energy than they emit due to the non-radiative energy dissipation, thus the absorbance maxima are at lower wavelengths than their corresponding emission maxima. Figure S3 shows the positive linear relationship between emission and absorbance maxima, with an R^2 value of 0.9879. It was expected¹¹ that the Stokes shift would remain mostly constant, and the slope of the data in Figure S3 would be close to 1. However, the slope was 0.7304, indicating that the Stokes shift decreases with increasing particle size as the absorbance peak position increases more than the emission peak position. It should be noted, however, that some absorbance maxima in the dataset were estimated because they were not well-defined, which is a possible source of error.

Quantum yield is a measure the efficiency of the photoluminescence process. The numerical value represents the ratio of photons absorbed that are re-emitted. A high quantum yield means that most or all the absorbed photons are re-emitted. Non-radiative relaxation processes decrease the quantum yield because photons are not emitted in these relaxation processes. In this experiment, the quantum yield of Sample 1 was calculated by comparison to the known quantum yield (0.65)¹² of the standard, Rhodamine B. The absorbance spectrum was collected for Sample 1 and Rhodamine B (Figure S4), and the lowest wavelength at which both samples absorb the same amount of light was chosen as the excitation wavelength, which was 510 nm. The emission spectra were collected for Sample 1 and Rhodamine B (Figure S5) using 510 nm as the excitation wavelength. The emission spectra were integrated to determine the photon flux for the standard and Sample 1, and correction factors were applied to account for small variations in absorbances and the refractive indices of the solvents. The quantum yield of Sample 1 was calculated (Calculation S1) to be 0.0495, meaning that 4.95% of photons absorbed were re-emitted in the relaxation process. This low yield means that Sample 1 is not a very efficient light emitter due to non-radiative energy emission. Quantum yield is affected by many factors, including temperature, solvent, and pH. The quantum yield could be improved by using solvents with higher viscosity, which decreases the rate of non-radiative relaxation.¹³

Transmission Electron Microscopy

Samples 1,4, and 6-9 of CdSe QDs were analyzed by transmission electron microscopy (TEM). While absorbance and emission spectra provide information used to make

conclusions about energy gaps, quantum yield, and trends in size, the actual size of the QDs is not easily determined from spectrophotometric methods, nor are details about their crystal structure revealed. Qualitatively, low-resolution TEM images revealed the shapes, uniformity, and separation of QDs. The dots were mostly well-separated and had spherical shapes, however, some appeared elongated. The elongation and clumping of dots were more prominent in samples withdrawn at later times. The low-resolution TEM images were used to determine the particle sizes for each sample by measuring 120 particles on ImageJ software for Samples 1, 4, and 6-9. The results are summarized in Table S2, and the size-distribution histograms are Figures S7-S12. Based on provided emission and absorption spectra, the theoretical radii of the particles were calculated⁷ (Calculation S2). Their sizes ranged from 2.55 nm (Sample 1) to 3.15 nm (Sample 8). The theoretical size of Sample 9 was smaller than that of Sample 8, and the TEM-measured sizes agreed with this prediction. The actual average sizes ranged from 2.20-3.77 nm with wide distributions. The measured sizes of the nanoparticles were larger than theoretical calculations, except for Sample 1 and 4, which had theoretical sizes that were overestimated by 16% and 4%, respectively. TEM measurements can confirm or disprove the validity of the particle-in-a-box model by comparing actual measured QD sizes to the theoretical sizes based on the Brus equation, as mentioned previously. The Brus equation overestimates the size of smaller QDs, so TEM can more accurately quantify the radii of smaller dots. The full width at half-maximum (FWHM) values in Table S2 quantify how broad the emission peaks are. Narrow emission peaks are desired for semiconducting materials because this means they produce high-colour-purity light, which is required for displays.¹⁴ These samples have mostly consistent peak widths (FWHM = 40-42 nm) except for Sample 1 and Sample 9, which have broader peaks. (FWHM = 52 and 74, respectively). All of the CdSe samples have FWHM values that are higher than the desired narrow (>30 nm)¹⁴ FWHM, suggesting that these QD samples do not produce very high-colour-purity light.

High-resolution TEM revealed information about the internal, crystalline structure of the QDs. The *d*-spacing, which is the distance between planes of atoms in a crystal lattice, was determined using the Fast Fourier transform (FFT) of the HRTEM image (Figure S6). FFT is a mathematical operation which breaks a HRTEM image up into its frequencies. FFT processes the data in HRTEM to provide meaningful information about the crystal lattice by reducing the grid-like pattern in the crystal structure HRTEM image to bright spots, which represent peaks. The bright spot corresponds to a periodic feature in the image that repeats, and returns the *d*-spacing value of the CdSe crystalline core. The *d*-spacing for three particles were 1.6, 1.6, and 1.8 Å. These spacings are in good agreement with literature value of 1.84 Å,¹⁵ but variations may be due to measurement angle.

CONCLUSION

CdSe quantum dots ranging from 2.20 to 3.77 nm in average radius, as measured by TEM, were synthesized by hot injection colloidal synthesis using a CdO and TOP-Se precursor. The QDs grew logarithmically over time and resulted in a red shift in absorbance and emission spectra due to quantum confinement. The Stokes shifts for the samples ranged from 16-40 nm, decreasing with increasing QD size. The

quantum yield of Sample 1 was 4.5%. The *d*-spacing of three synthesized dots were 1.6, 1.6, and 1.8 Å, which agreed with literature reports. Future experiments could alter pH or solvents to obtain a better quantum yield and investigate ways to produce QDs with a narrower size distribution.

EXPERIMENTAL

The procedures for this experiment were followed as outlined in the Chemistry 3LA3 Manual.¹⁶

REFERENCES

- (1) A. Cotta, M. Quantum Dots and Their Applications: What Lies Ahead? *ACS Appl. Nano Mater.* **2020**, 3 (6), 4920–4924.
- (2) Subila, K. B.; Kishore Kumar, G.; Shivaprasad, S. M.; George Thomas, K. Luminescence Properties of CdSe Quantum Dots: Role of Crystal Structure and Surface Composition. *J. Phys. Chem. Lett.* **2013**, 4 (16), 2774–2779.
- (3) L. Landry, M.; E. Morrell, T.; K. Karagounis, T.; Hsia, C.-H.; Wang, C.-Y. Simple Syntheses of CdSe Quantum Dots. *J. Chem. Educ.* **2014**, 91 (2), 274–279.
- (4) Gao, Y.; Peng, X. Crystal Structure Control of CdSe Nanocrystals in Growth and Nucleation: Dominating Effects of Surface versus Interior Structure. *J. Am. Chem. Soc.* **2014**, 136 (18), 6724–6732.
- (5) Mohamed, M. B.; Tonti, D.; Al-Salman, A.; Chemseddine, A.; Chergui, M. Synthesis of High Quality Zinc Blende CdSe Nanocrystals. *J. Phys. Chem. B* **2005**, 109 (21), 10533–10537.
- (6) Hao, E.; Sun, H.; Zhou, Z.; Liu, J.; Yang, B.; Shen, J. Synthesis and Optical Properties of CdSe and CdSe/CdS Nanoparticles. *Chem. Mater.* **1999**, 11 (11), 3096–3102.
- (7) Salem, A.; Saion, E.; Al-Hada, N. M.; Mohamed Kamari, H.; Shaari, A. H.; Abdullah, C. A. C.; Radiman, S. Synthesis and Characterization of CdSe Nanoparticles via Thermal Treatment Technique. *Results Phys.* **2017**, 7, 1556–1562.
- (8) Murray, C. B.; Norris, D. J.; Bawendi, M. G. Synthesis and Characterization of Nearly Monodisperse CdE (E = S, Se, Te) Semiconductor Nanocrystallites. *J. Am. Chem. Soc.* **1993**, 115, 8706–8715.
- (9) Meyns, M.; Iacono, F.; Palencia, C.; Geweke, J.; Coderch, M. D.; Fittschen, U. E. A.; Gallego, J. M.; Otero, R.; Juárez, B. H.; Klinke, C. Shape Evolution of CdSe Nanoparticles Controlled by Halogen Compounds. *Chem. Mater.* **2014**, 26 (5), 1813–1821.
- (10) Khanna, P. K.; Morley, C. P.; Gorte, R. M.; Gokhale, R.; Subbarao, V. V. S.; Satyanarayana, C. V. V. A Simple and Effective Synthesis of Cadmium Selenide in Aqueous N,N'-Dimethylformamide. *Mater. Chem. Phys.* **2004**, 83 (2–3), 323–327.
- (11) J. Nordell, K.; M. Boatman, E.; C. Lisensky, G. A Safer, Easier, Faster Synthesis for CdSe Quantum Dot Nanocrystals. *J. Chem. Educ.* **2005**, 82 (11).
- (12) Kubin, R. F.; Fletcher, A. N. Fluorescence Quantum Yields of Some Rhodamine Dyes. *J. Lumin.* **1982**, 27 (4), 455–462.
- (13) Omary, M. A.; Patterson, H. H. Luminescence, Theory. *Encycl. Spectrosc. Spectrom.* **2017**, 636–653.
- (14) Kawamura, M.; Kuwae, H.; Kamibayashi, T.; Oshima, J.; Kasahara, T.; Shoji, S.; Mizuno, J. Liquid/Solution-Based Microfluidic Quantum Dots Light-Emitting Diodes for High-Colour-Purity Light Emission. *Sci. Reports* **2020**, 10 (1), 1–9.
- (15) Patel, K. D.; Shah, R. K.; Makhija, D. L.; Pathak, V. M.; Srivastava, R. Chemical And Structural Characterization of CdSe Thin Films. *J. Ovonic Res.* **2008**, 4 (6), 129–139.
- (16) Chemistry 3LA3 Laboratory Manual, *Project 2: Synthesis and characterization of chalcogenide quantum dots*; McMaster University: Hamilton, ON, 2021.

Supporting Information

Table of Contents

Figure S1. Normalized absorbance spectra of nine CdSe colloid fractions (Set A)	S2
Figure S2. Normalized emission spectra of nine CdSe colloid fractions (Set A).....	S3
Figure S3. Graph of maximum absorbance and maximum emission wavelengths (Set A).....	S3
Figure S4. Sample 1 and Rhodamine B absorbance spectrum for quantum yield.....	S4
Figure S5. Sample 1 and Rhodamine B emission spectrum for quantum yield	S4
Table S1. Data for Quantum Yield Calculation.....	S5
Calculation S1. Quantum Yield Calculation.....	S5
Table S2. Summary of CdSe quantum dot sizes and emission peaks.....	S5
Calculation S2. Sample Calculation of Theoretical Radius.....	S5
Figure S6. First FFT of CdSe HRTEM Image.....	S6
Figure S7-12. Size distribution histograms of six quantum dot samples	S7-9

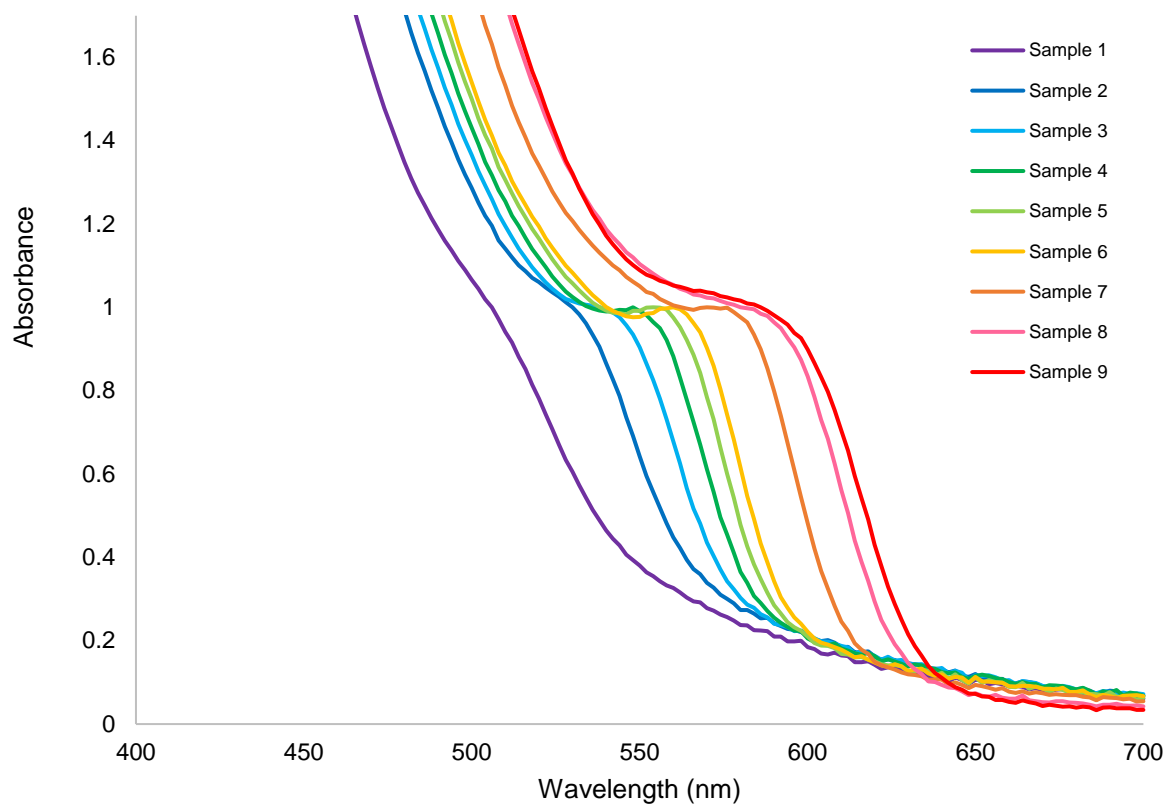


Figure S1. Normalized absorbance spectra of nine CdSe colloid fractions from Set A from $\lambda = 400$ -700 nm. The interval was 2.0 nm, and the speed was fast.

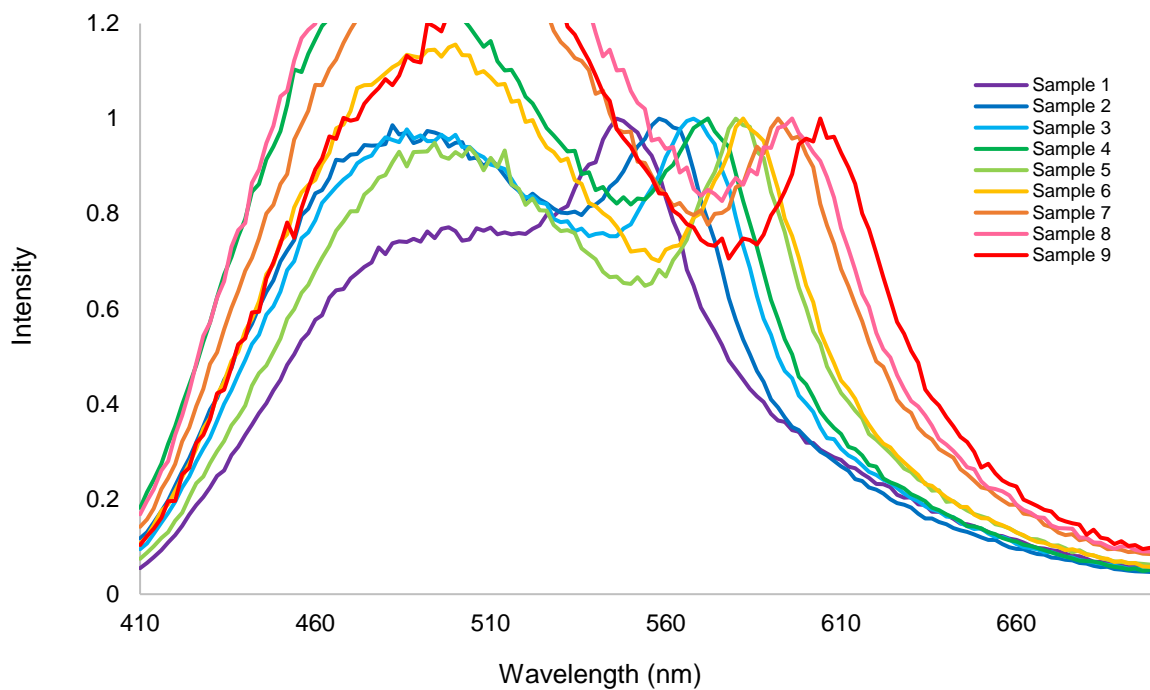


Figure S2. Normalized emission spectra of nine CdSe colloid fractions from $\lambda = 410$ -700 nm. The excitation wavelength was 400 nm.

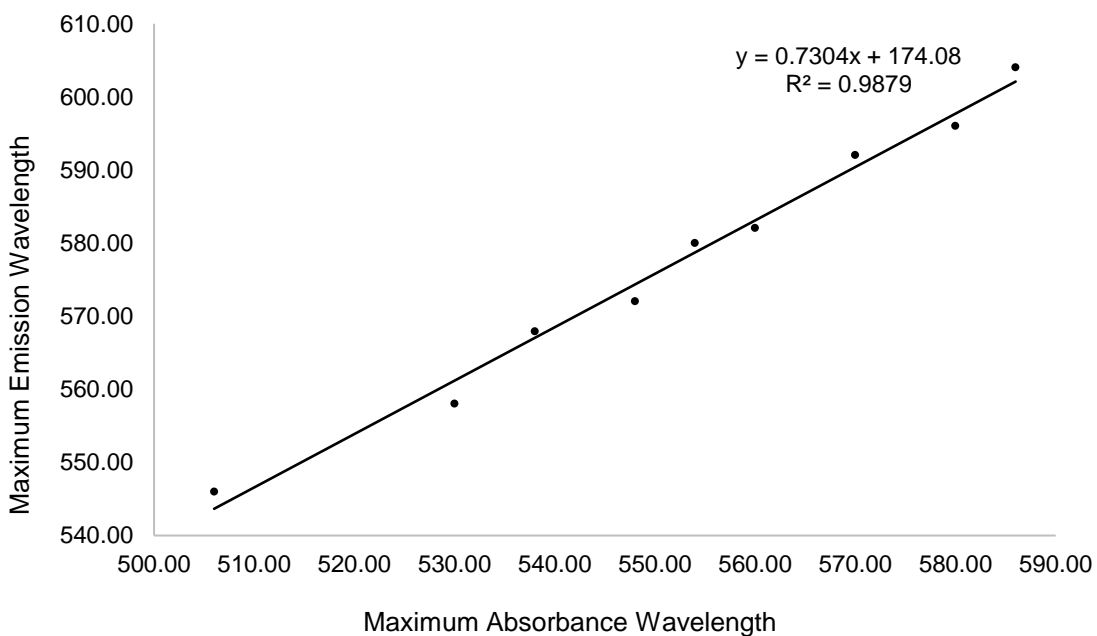


Figure S3. Plot of maximum emission wavelength vs corresponding maximum absorbance wavelength for each of the nine CdSe colloids. Points with higher absorbance/emission are samples withdrawn at later times. A strong positive linear correlation between maximum absorbance and emission.

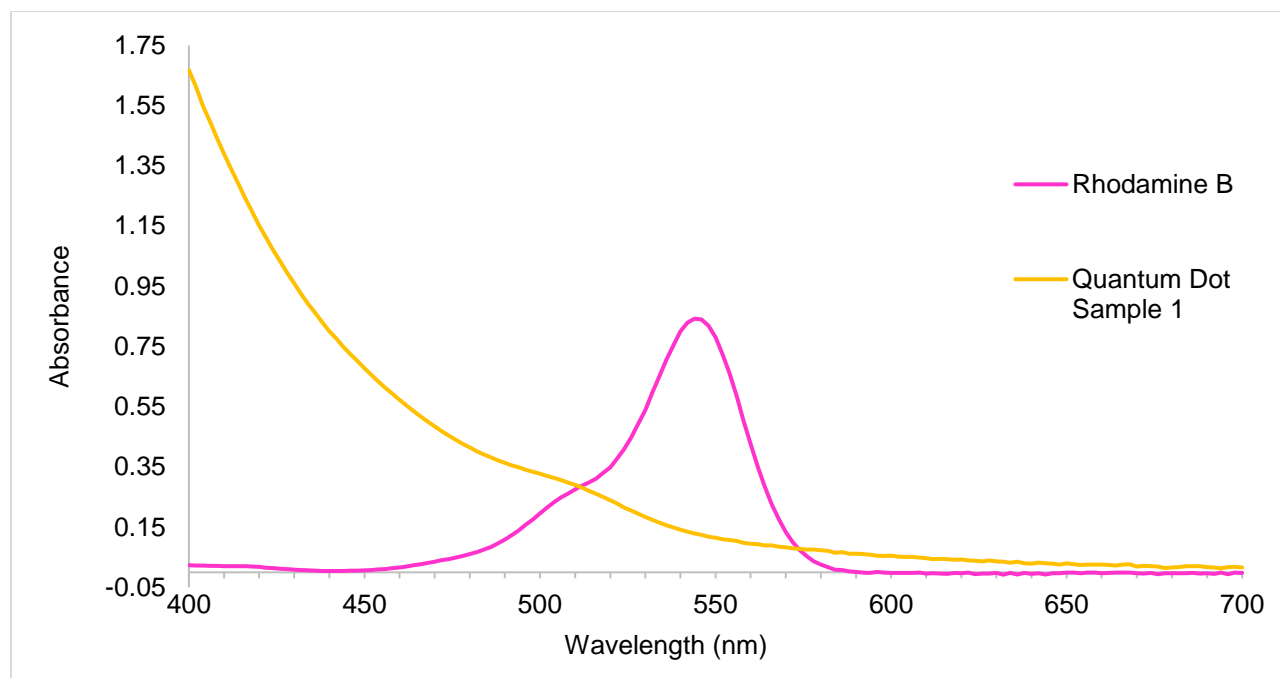


Figure S4. Absorbance spectra of rhodamine B standard and CdSe colloid sample 1. The interval was 2.0 nm, and the speed was fast. Ethanol was the blank for rhodamine B and a mixture of oleic acid and octadecene was the blank for sample 1.

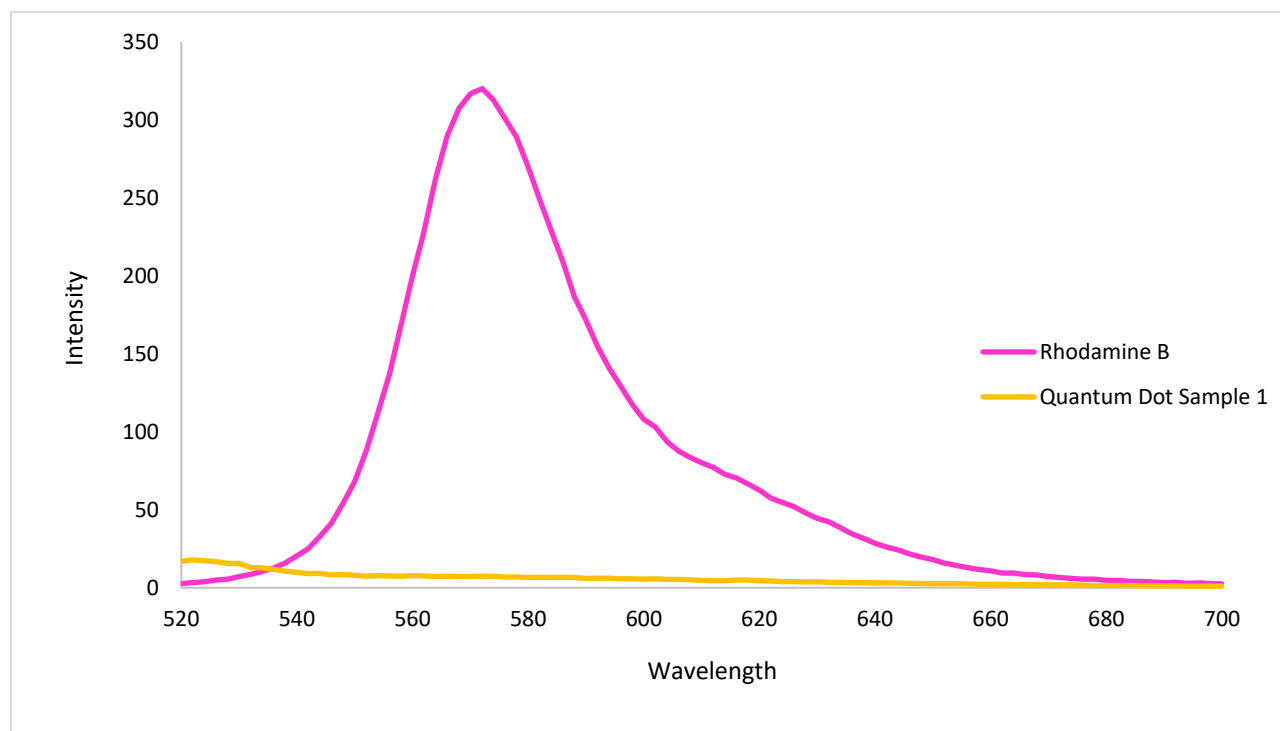


Figure S5. Emission spectra of rhodamine B standard and CdSe colloid sample 1. The slit widths were 2.5 nm, and the excitation wavelength was 510 nm.

Table S1. Data for Sample 1 and Rhodamine B Absorbance/Emission Spectra

Sample	Absorbance at 510 nm	Absorbance Correction Factor	Integrated Photon Flux	Solvent Refractive Index
Rhodamine B	0.27564	0.46990	8326043.161	1.361
Quantum Dot Sample 1	0.28983	0.48694	583526.891	1.444

Calculation S1. Quantum Yield Calculation

Quantum yield of Rhodamine B¹²: 0.65

$$\begin{aligned}
 \phi_1 &= \phi_{st} \left(\frac{F_x}{F_{st}} \right) \left(\frac{f_{st}}{f_x} \right) \left(\frac{n_x^2}{n_{st}^2} \right) \\
 &= 0.65 \times \frac{583526.891}{8326043.161} \times \frac{0.46990}{0.48694} \times \frac{1.444^2}{1.361^2} \\
 &= 0.0495 \\
 &= 4.95\%
 \end{aligned}$$

Table S2. Summary of CdSe quantum dot sizes (radii) and emission peaks

Sample	Emission λ_{max} (nm)	Theoretical Size (nm)	Actual Size (n= 120, (nm)	Full Width at Half Max (nm)	Size Distribution (nm)
1	536	2.55	2.20	52	1.22-3.53
4	564	2.85	2.74	40	1.38-4.62
6	570	2.93	3.26	42	1.32-5.40
7	577	3.02	3.34	42	1.78-5.35
8	586	3.15	3.77	42	1.41-6.36
9	577	3.02	3.71	74	1.69-5.61

Calculation S2. Theoretical radius of CdSe Sample 1 quantum dots.

$$\begin{aligned}
 r &= \sqrt{\frac{h^2 \left(\frac{1}{m_e^*} + \frac{1}{m_h^*} \right)}{8 \left(\frac{hc}{\lambda} - E_{gap} \right)}} \\
 &= \sqrt{\frac{(6.63 \times 10^{-34} Js)^2 \left(\frac{1}{1.18 \times 10^{-31} kg} + \frac{1}{4.10 \times 10^{-31} kg} \right)}{8 \left(\frac{6.63 \times 10^{-34} Js \times 3.00 \times \frac{10^8 m}{s}}{5.36 \times 10^{-7} m} - 2.79 \times 10^{-19} J \right)}} \\
 &= 2.55 \text{ nm}
 \end{aligned}$$

Note: Bulk bandgap of CdSe, E_{gap} , is 1.74 eV, or $2.79 \times 10^{-19} \text{ J}$.⁷

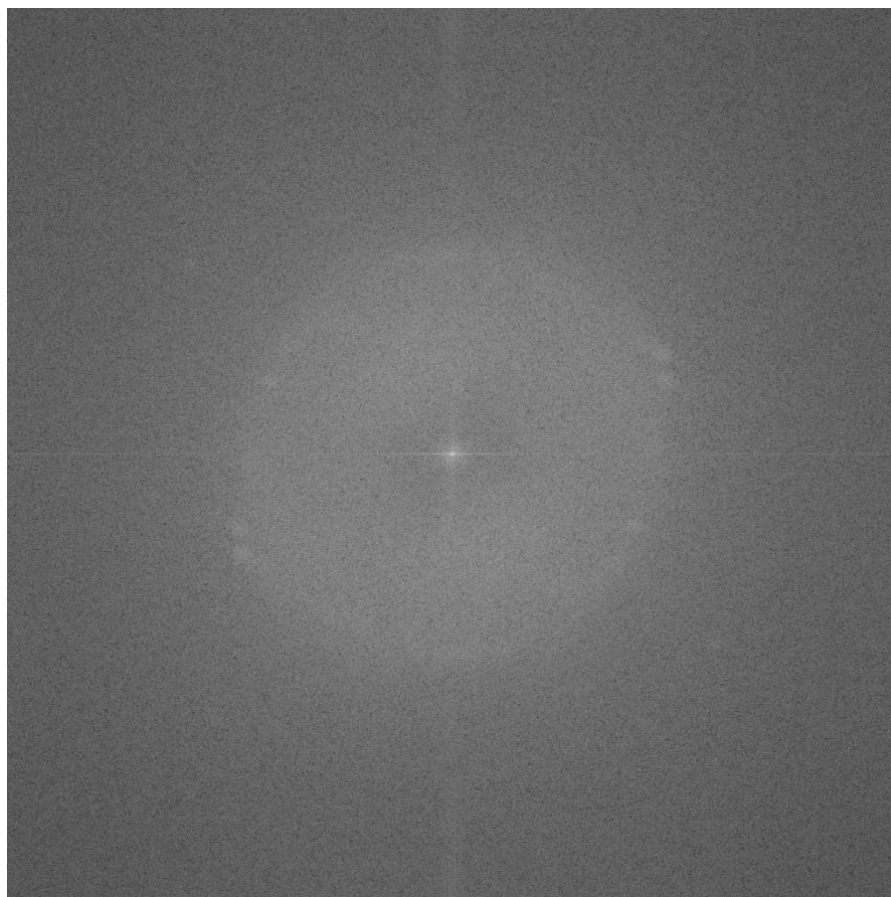


Figure S6. Fast Fourier transform of high-resolution transmission electron microscopy image of the first CdSe quantum dot particle used to determine the d -spacing, which was 0.16 nm.

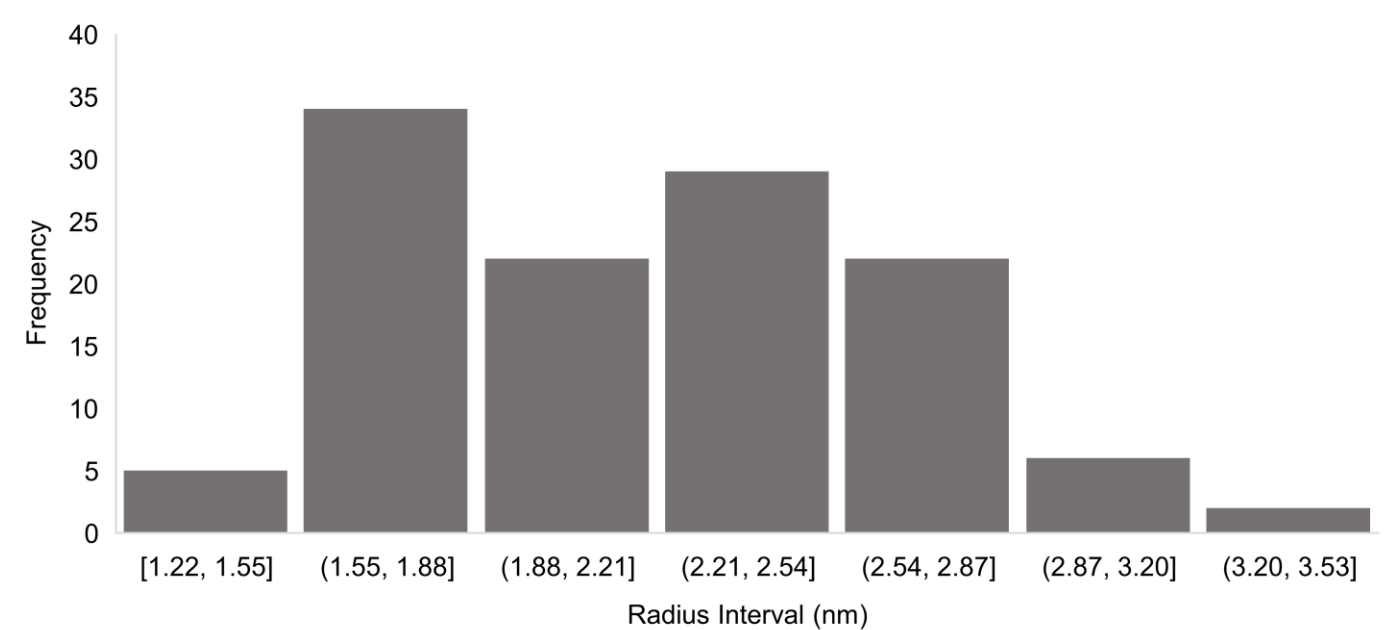


Figure S7. CdSe particle size distribution (n=120) for Sample 1. Measurements were made using TEM. Data collected from Kirsten Entz, Jaime Ciere, Tanjot Grewal, and Claire Gillespie.

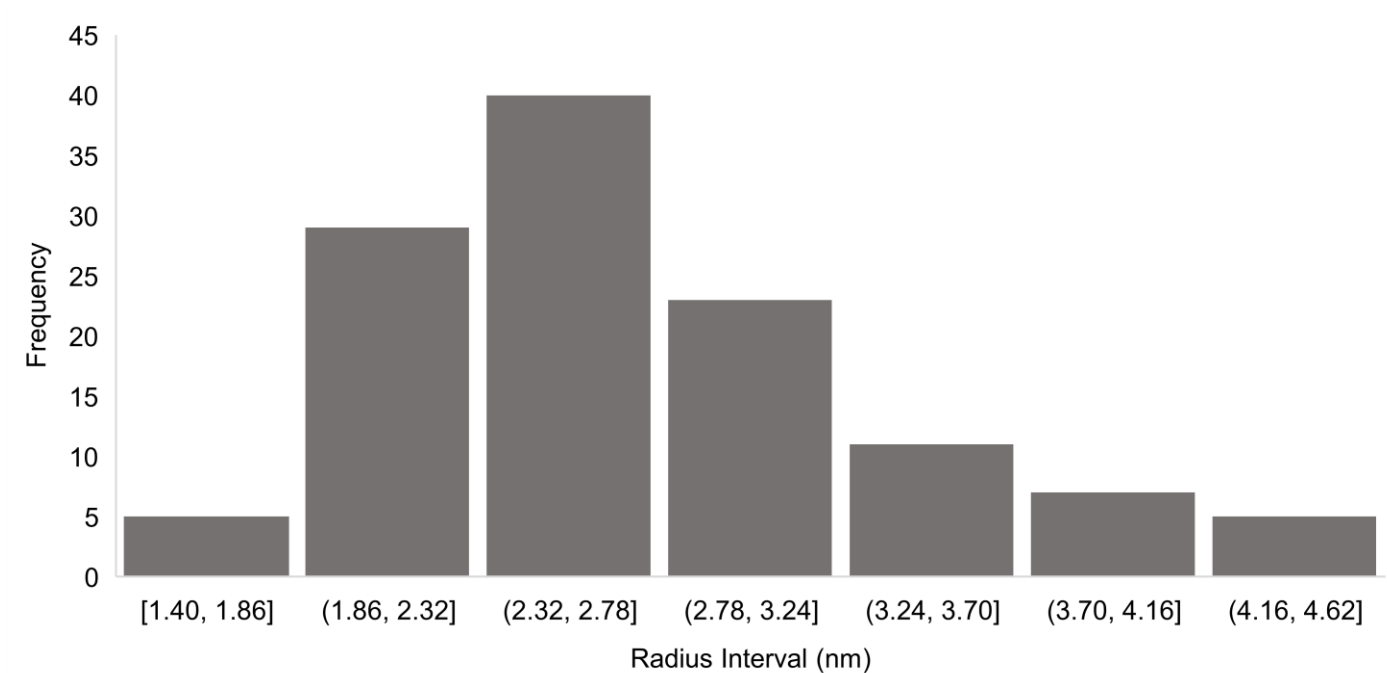


Figure S8. CdSe particle size distribution (n=120) for Sample 4. Measurements were made using TEM. Data collected from Kirsten Entz, Jaime Ciere, Tanjot Grewal, and Claire Gillespie.

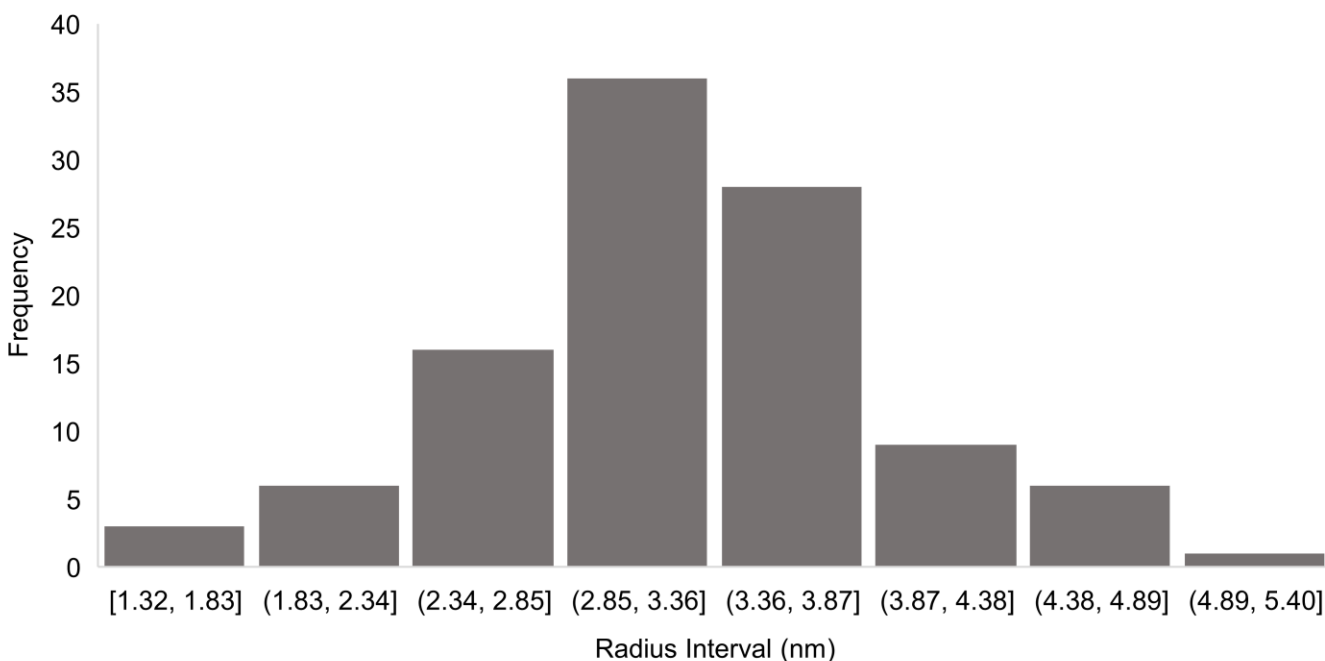


Figure S9. CdSe particle size distribution (n=120) for Sample 6. Measurements were made using TEM. Data collected from Kirsten Entz, Jaime Ciere, Tanjot Grewal, and Claire Gillespie.

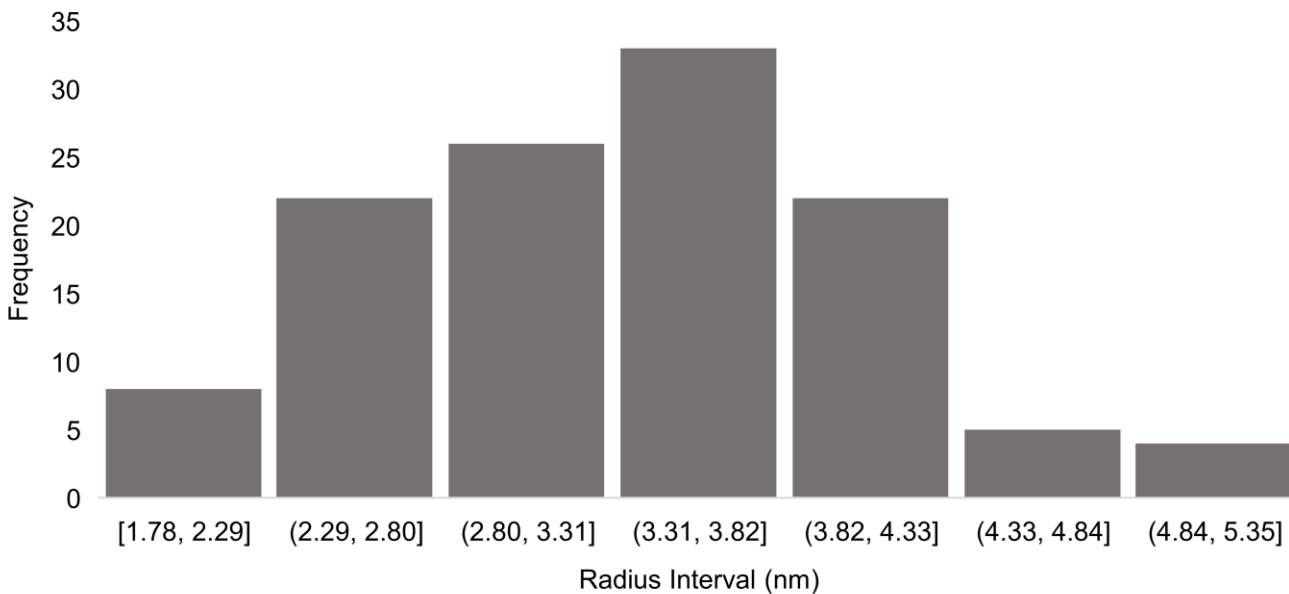


Figure S10. CdSe particle size distribution (n=120) for Sample 7. Measurements were made using TEM. Data collected from Kirsten Entz, Jaime Ciere, Tanjot Grewal, and Claire Gillespie.

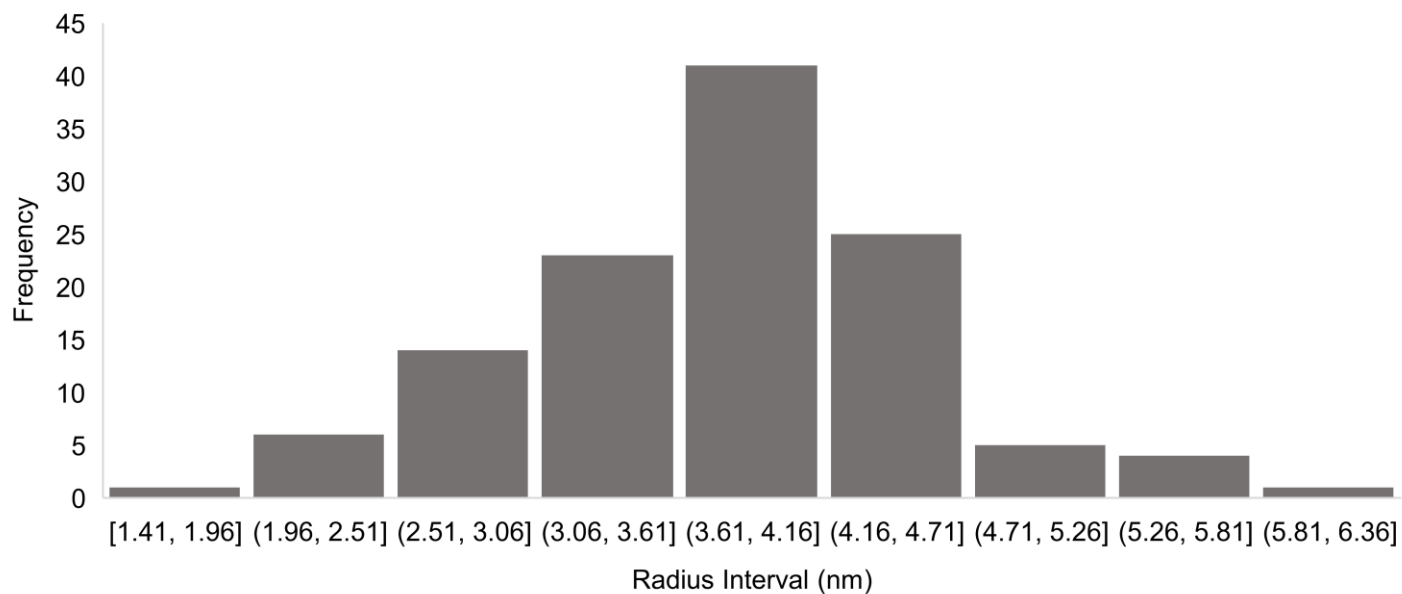


Figure S11. CdSe particle size distribution (n=120) for Sample 8. Measurements were made using TEM. Data collected from Kirsten Entz, Jaime Ciere, Tanjot Grewal, and Claire Gillespie.

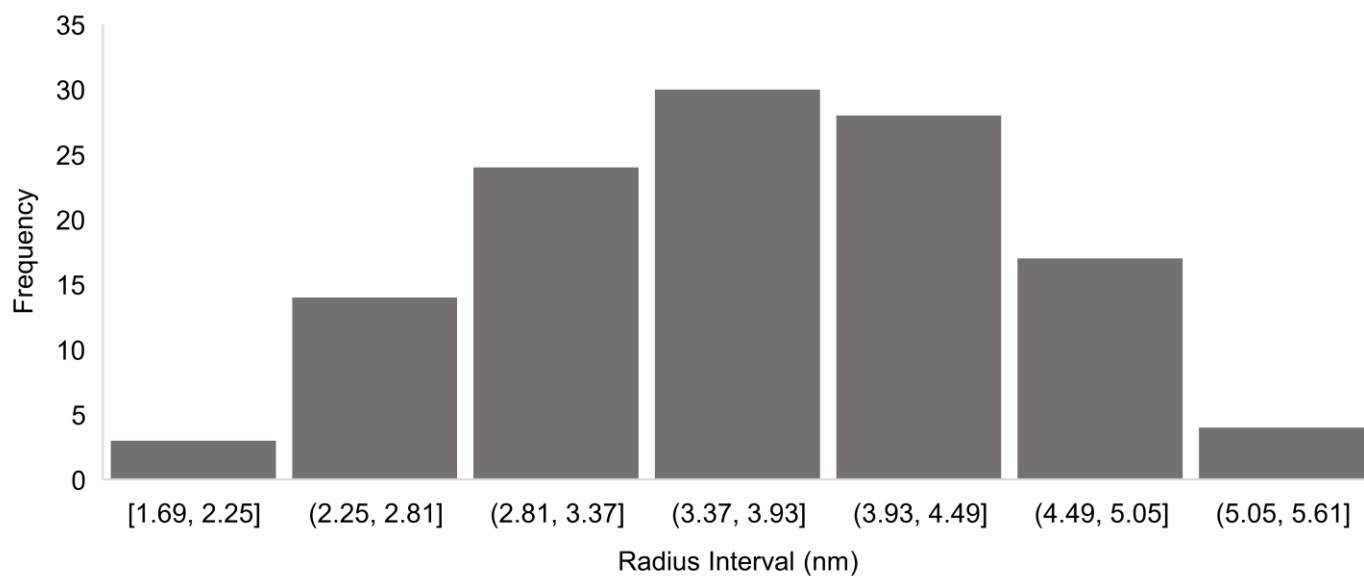


Figure S12. CdSe particle size distribution (n=120) for Sample 9. Measurements were made using TEM. Data collected from Kirsten Entz, Jaime Ciere, Tanjot Grewal, and Claire Gillespie.